

Detection of Brain Tumor Using Zernike Moments on Magnetic Resonance Images

Kiran Thapaliya and Goo-Rak Kwon

Department of Information and Communication Engineering

Chosun University

Gwangju, South Korea

{kiranthapaliya9@gmail.com, grkwon@chosun.ac.kr}

Abstract- In this study, a new method has been developed for the detection of brain tumor in magnetic resonance images. Magnetic resonance images are analyzed using the Zernike moments and different orders of Zernike moments are calculated. The image is divided into two parts from the center of the image. The average value of the pixels located at the central line is calculated. The new vectors of the pixel are formed based on the calculated average value. The value obtained from the low and high order of Zernike moments are used to calculate the proper threshold value which can extract the tumor efficiently. The proposed method was tested with the different magnetic resonance images containing tumor and the algorithm was successful to analyze the tumor part from the brain image.

Keywords- Zernike moments; Zernike polynomials; Mean; MRI; Segmentation.

I. INTRODUCTION

According to the data of World Health Organization (WHO), more than 400000 persons take the treatment of brain tumor every year [29]. Treatment of brain tumor is a difficult task. It is believed that a careful diagnosis might save patients life. The segmentation of brain tumor from Magnetic Resonance Images (MRI) is a difficult task that involves several disciplines such as pathology, MRI physics, radiologist's perception, and image analysis based on intensity, shape and size. There are several issues and challenges in proper segmentation of brain tumor. Tumors differ with shape, size and location and varies with their intensity. The accurate segmentation of brain tumor is of great interest. Most patients in hospital undergo Computerised Tomography (CT) scan and MRI for the identification of tumor part in the brain. Manual segmentation is risky most of the time and may create problem during the diagnosis by naked eye. Therefore, it is always necessary to use an automatic method to extract the tumor part of the brain; this reduces the human error.

Different methods and approaches have been proposed for the extraction of brain tumor. Some methods are manual, others are semi-automatic and others are automatic. Fuzzy, clustering, edge detection, region growing, and level set methods are introduced in the field of segmentation. Clustering-based methods, such as K-means clustering, have a fast speed even on large datasets but they doesn't provide the same result in each run due to their dependency on initial random assignments [1-2]. Hierarchical self-organizing map- based multiscale image segmentation [3]

and 3D variational segmentation-based methods [4] were also used for the image segmentation [5,6].

These methods used artificial intelligence techniques for automated tumor segmentation. Statistical pattern recognition based methods [7,8-10] fall short, partly because large deformations occur in the intracranial tissues due to the growth of the tumor and edema. However, these techniques need to significantly modify the brain atlas to accommodate the tumors, which specially lead to poor results. The method presented by Singh and Dubey method [27] used the marker based watershed approach to segment the tumor, but it is not an efficient method because it loses tumor information and it is time consuming. Most researchers are using Markov random fields (MRFs) [11,12], which involve estimating the parameters for a parametric model that has one set of parameters to express the probability that each specific voxel is a tumor, and another set to express the distribution over the labels for a pair of adjacent voxels. In Gray Level Co-occurrence Matrix (GLCM) method [14], there is an inherent problem to choose the optimal inter-pixel distance in a given situation. Zernike moments are the mapping of an image onto a set of complex Zernike polynomials [15]. J.K. Udupa et al. [16] combined morphological process and the region growing methods in order to determine tumor volume. Based on the fuzzy logic, Khotanzad and Hong[17] used the fuzzy clustering or the fuzzy connectedness for addressing the problem of abnormal tissue segmentation and classification. Some authors [18-21] used Zernike moments and implemented in the area of image analysis. Zernike polynomials are orthogonal to each other. Zernike moments can represent the properties of an image with no redundancy or overlap information between the moments [22]. Due to these properties, Zernike moments have been widely used in different types of applications [15]. Zernike moments have been used in shape based image retrieval [23], feature set [24] and edge detection in pattern recognition [25]. Even though Zernike moments are used in various fields, they have drawbacks of computational complexity that make unsuitable for real time application.

In this paper, a new method has been developed for the diagnosis of the MR images containing tumor. The main aim of the paper is to extract the tumor part efficiently from MR images and reduce human manual interaction. The detail of Zernike moments has been described in section II, the detail algorithm for the extraction of brain tumor has

been described in section III, followed by the experimental results and conclusion in section IV and V respectively.

II. ZERNIKE MOMENTS

Zernike moments are based on complex polynomials that form a complete orthogonal set on a unit circle. The Zernike moments over the unit circle $x^2 + y^2 = 1$ is described by

$$v_{nm} = v_{nm}(\rho, \theta) = R_{nm}(\rho) e^{im\theta} \quad (1)$$

where, n is a non-negative integer and m is a non-zero integer, under the condition $n - |m|$ is even and $|m| \leq n$, and ρ is a vector from the origin of the disc to a point on it. θ is the angle that the vector ρ makes with the positive direction of x-axis in the counter clockwise direction. $R_{nm}(\rho)$ are the Zernike radial polynomials in polar coordinates and are defined by

$$R_{nm}(\rho) = \sum_{s=0}^{(n-|m|)/2} (-1)^s \frac{(n-s)!}{s! \left(\frac{n+|m|}{2} - s\right)! \left(\frac{n-|m|}{2} - s\right)!} \rho^{n-2s} \quad (2)$$

Polynomials in above equation are orthogonal and according to orthogonality condition

$$\int \int_{x^2+y^2 \leq 1} v_{nm}^*(x, y) v_{pq}(x, y) dx dy = \frac{\pi}{n+1} \delta_{np} \delta_{mq} \quad (3)$$

where, $\delta_{np} = 1$ when $n = p$ and zero otherwise. δ_{np} and δ_{mq} is the Kronecker delta.

Zernike functions corresponding to continuous function $f(x, y)$. Zernike moment for order n and repetition m is given by

$$A_{nm} = \frac{n+1}{\pi} \int \int_{x^2+y^2 \leq 1} f(x, y) v_{nm}^*(\rho, \theta) dx dy \quad (4)$$

If $f(x, y)$ is a digital image, we replace the integral by summations to get Zernike moments for the image. Then,

A_{nm} , in this case, reduces to

$$\begin{aligned} A_{nm} &= \frac{n+1}{\pi} \sum_x \sum_y f(x, y) v_{nm}^*(\rho, \theta) \\ &= \frac{n+1}{\pi} \sum_{\rho=0}^1 \sum_{\theta=0}^{2\pi} f(\rho, \theta) R_{nm}(\rho) e^{-im\theta} \\ &= \frac{n+1}{\pi} \sum_{\rho=0}^1 R_{nm}(\rho) \sum_{\theta=0}^{2\pi} f(\rho, \theta) e^{-im\theta} \end{aligned} \quad (5)$$

III. PROPOSED METHOD

In this paper, the value of low and high order Zernike moments are used to segment the tumor from the MR images. The input image is divided into two parts with different pixels value. The division of pixel is performed

vertically from the center of the image. The low order and high order Zernike moments are calculated using Equ. (5). The values of low and high order Zernike polynomials are used to calculate low and high order of Zernike moments respectively. In the proposed method, different values of Zernike moments are calculated at different order. Thus, obtained value is utilized to calculate the mean value, which separates the tumor from the image. The detail procedure for extraction of tumor image is discussed in the following section.

A. Feature extraction and Selection

The image is divided into two left and right hemispheres. These two hemispheres of the image contain complex Zernike moment value. The division of pixel is based on the average value of the pixels located at the center boundary of image.

Let us assume that $f(x, y)$ is the image formed by the complex Zernike moments value. $b(x, y)$ is the image pixels located at the center boundary of image. We calculate the average value of the pixel $b(x, y)$ located at the center boundary of the image as shown in the fig. (1). Average pixel value is calculated using following equation.

$$Avgvalue = \frac{1}{N} \sum_{x=0}^{x=x-1} \sum_{y=0}^{y=y-1} b(x, y) \quad (6)$$

where, N is the total number of pixels located at the center boundary of the image.

The image is divided into left and right hemisphere; choose the minimum pixel values (that is not zero) from the left hemisphere of the divided image. Thus, form vector of all the pixels that lies between minimum values of the left hemisphere of the image to the average value *Avgvalue* of the boundary. Similarly, choose the minimum value of pixel from the right hemisphere of the image to the average value *Avgvalue* of the center boundary of the image. Thus, vector form is the range of minimum pixel value from the left and right hemisphere to the average value of central boundary pixel. These pixels vector are combined together and treated as a single image $k(x, y)$. $I_1(x_n, y_n)$ is the range of pixel values from left hemisphere to the average pixel value *Avgvalue* of the pixel located at the center boundary. Similarly, $I_2(x_n, y_n)$ is the range of pixel values from right hemisphere to the average pixel value *Avgvalue* of the pixel located at the center boundary. $k(x, y)$ is the vector formed from the pixel $I_1(x_n, y_n)$ and $I_2(x_n, y_n)$

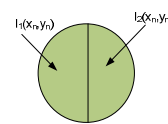


Fig.1. Division of image into two parts from the center of the image

The low order and high order Zernike moments are calculated for the different order N and with repetition of M of the image. The table below shows the low and high order Zernike moments for the image.

TABLE I. SAMPLE ORDER REPETITION COMBINATION

Group	N	M	Number of moments
Low order Zernike moments	2	0,2	18
	3	1,3	
	4	0,2,4	
	5	1,3,5	
	6	0,2,4,6	
High order Zernike moments	7	1,3,5,7	18
	7	3,7	
	8	0,4,8	
	9	1,5,9	
	10	2,6,10	
	11	3,7,11	
	12	0,4,8,12	

In, the table above, 18 Zernike moments are selected for the low and high order Zernike moments that satisfy the following conditions

$$LZM = \{Z_{n,m}\} \forall \begin{cases} 2 \leq n \leq 7 \\ |m| \leq n \\ n - |m| = 2k \\ k \in N \end{cases} \quad (7)$$

$$HZM = \{Z_{n,m}\} \forall \begin{cases} 7 \leq n \leq 12 \\ |m| \leq n \\ n - |m| = 4k \\ k \in N \end{cases}$$

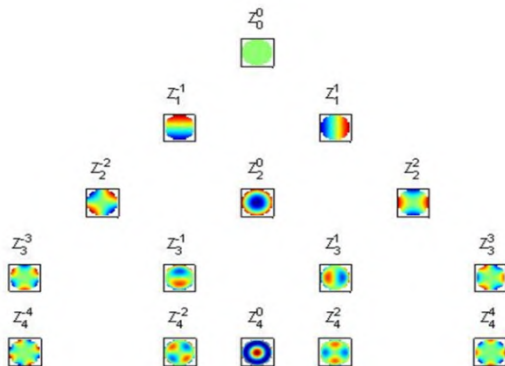


Fig.2. Plots of the magnitude of low order Zernike basis function in the unit disk.

B. Segmentation

The final step of the proposed method is the extraction of tumor from the image. The vectors contain the complex Zernike moment value; we calculate the appropriate thresholding value, which can separate the tumor from the image using these complex Zernike moments value. Complex Zernike moments value contain low order Zernike moments and high order Zernike moments. Here, we calculate the mean value for each real and imaginary part of low order Zernike moments separately. Similarly, the calculation of mean value for real and imaginary part for high order complex Zernike moments are carried out separately.

$$\mu_1 = \left\{ \max \left(\frac{1}{x \times y} \sum_{x=0}^{x-1} \sum_{y=0}^{y-1} k_1(x, y) \right) \right\}^{\frac{1}{2}}$$

$$\mu_2 = \left\{ \max \left(\frac{1}{x \times y} \sum_{x=0}^{x-1} \sum_{y=0}^{y-1} k_2(x, y) \right) \right\}^{\frac{1}{2}} \quad (8)$$

$$\mu_3 = \left\{ \max \left(\frac{1}{x \times y} \sum_{x=0}^{x-1} \sum_{y=0}^{y-1} k_3(x, y) \right) \right\}^{\frac{1}{2}}$$

$$\mu_4 = \left\{ \max \left(\frac{1}{x \times y} \sum_{x=0}^{x-1} \sum_{y=0}^{y-1} k_4(x, y) \right) \right\}^{\frac{1}{2}}$$

where, μ_1 and μ_2 are the mean value of real and imaginary part of low order Zernike moment respectively. $k_1(x, y)$ and $k_2(x, y)$ are pixel values that contains only real and imaginary pixel values of low order Zernike moments respectively. μ_3 and μ_4 are the mean value of real and imaginary part of high order Zernike moments respectively. $k_3(x, y)$ and $k_4(x, y)$ are the pixel values that contains only real and imaginary pixel values of high order Zernike moments respectively.

Now, we subtract the mean value of real part of low order Zernike moments from real part of high order Zernike moments

$$\mu_5 = \mu_3 - \mu_1 \quad (9)$$

where, μ_5 is the mean value after subtracting two mean values of real part of low and high Zernike moments.

Similarly, we subtract the mean value of imaginary part of low order Zernike moments from imaginary part of high order Zernike moments which is given as

$$\mu_6 = \mu_4 - \mu_2 \quad (10)$$

where, μ_6 is the mean value after subtracting mean values of imaginary part of low and high Zernike moments

Now, we calculate the final thresholding value, which can separate the tumor from other objects in the image.

$$T = \frac{\mu_5 + \mu_6}{2} \tag{11}$$

$k(x,y)$ is the image that contains the low and high order Zernike moments value. Now using this thresholding value, we obtained only the tumor part from the image $k(x,y)$.

$$final(x,y) = \begin{cases} 1 & \text{if } k(x,y) \leq T \\ \text{else} & \\ 0 & \text{otherwise} \end{cases} \tag{12}$$

$final(x,y)$ is the final tumor part extracted from the image.

Finally, the replacement of the pixel is done to get the desired output tumor segmented image. The pixel replacement is performed as

$$\begin{aligned} \text{if } final(x,y) = 1 \text{ then } final(x,y) = 0 \\ \text{else otherwise } final(x,y) = k(x,y) \end{aligned} \tag{13}$$

IV. EXPERIMENTAL RESULTS

The proposed method was tested with different MR images. The proposed method was tested with the brain having different intensity, shape and size. The low order Zernike moments were calculated from different kinds of brain tumor images and proposed method was successful to efficiently extract the tumor part from the brain tumor images. The method was tested using MATLAB 2012. The images size of 240X240 for Fig. 3 and 200X200 for Fig. 4-7 was taken for the experimental purpose. Experimental results for the different kinds of images are shown below.

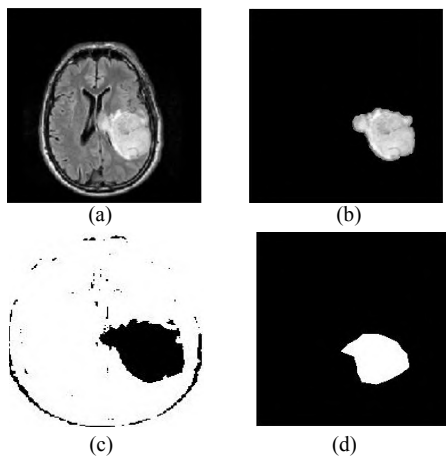


Fig. 3. Extraction of huge mass of brain tumor. (a) Original image, (b) extracted tumor from proposed method, (c) Region grows method, and (d) Singh and Dubey method.

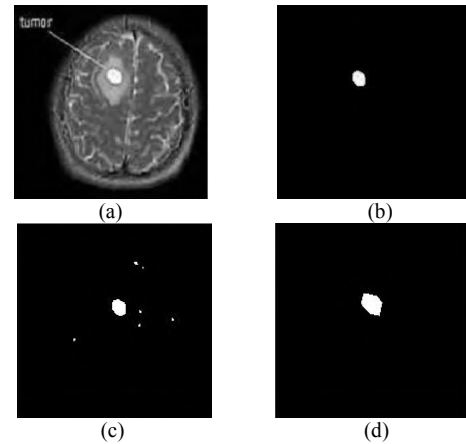


Fig. 4. Segmentation of tumor using proposed method. (a) Original image, (b) Segmented tumor from proposed method, (c) Region grows method, and (d) Singh and Dubey method.

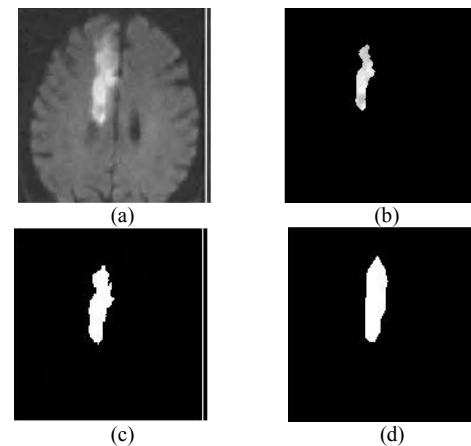


Fig. 5. Segmentation of brain tumor having cylindrical shape (a) Original image, (b) Proposed method, (c) Region grows method, and (d) Singh and Dubey method.

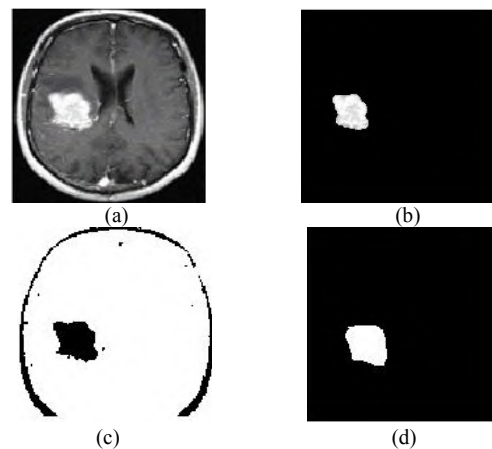


Fig. 6. Extracted star shaped tumor using our proposed method. (a) Original image, (b) Proposed method, (c) Region grows method, and (d) Singh and Dubey method

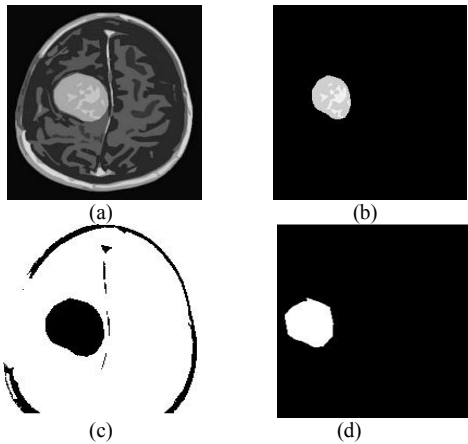


Fig. 7. Extracted oval shaped brain tumor. (a) Original image, (b) Proposed method, (c) Region grows method, and (d) Singh and Dubey method.

Fig. 3-7 show the different images obtained from the proposed method and other two methods, region grow and Singh and Dubey method. In Fig. 3 (a) is the original image with the huge mass of tumor. Fig. 3(b), (c) and (d) are the tumor images obtained by the proposed, region grow and Singh and Dubey method respectively. It is clear from the experimental results that the proposed method effectively extracts the tumor part accurately rather than other two methods. Similarly, from Figs. 4-7, the proposed method gives better results in comparison to other methods. Therefore, by subjective analysis it is clear that the proposed method outperforms the other two methods for the extraction of tumor part from the input brain MRI images.

To prove the proposed method is better than the region grows and Singh and Dubey method quantitatively, we calculate the Root Mean Square Error (RMSE) and time complexity.

Root mean square error (RMSE): it is a quadratic scoring rule which measures the average magnitude of the error. The RMSE value is calculated as

$$RMSE = \sqrt{\frac{\sum_{i=1}^n (Q_m - Q_A)^2}{n}} \quad (14)$$

where, Q_m and Q_A are the tumor voxels segmented manually and the different methods, respectively, and n is the size of the image.

RMSE value calculated for different images using different method is shown in Table II.

TABLE II. RMSE OF PROPOSED AND OTHER TWO METHODS

Figure	Proposed	Region grow	Singh and Dubey
Fig. 3	0.09	0.98	0.96
Fig. 4	0.05	1.25	0.99
Fig. 5	0.22	1.01	0.87
Fig. 6	0.20	1.31	0.97
Fig. 7	0.24	1.76	0.93

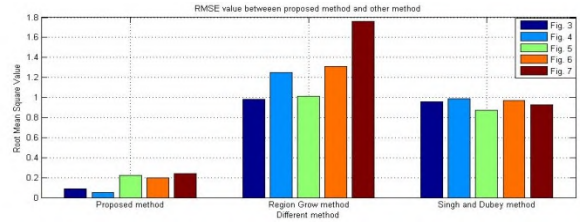


Fig. 8. RMSE value of proposed method and other two methods

The RMSE value of Table II is shown in graphical representation. From the above table and graph, it is clear that the RMSE value of the proposed method is less than the region grow and Singh and Dubey method. The data above clearly mentions that the proposed method is better than the other two methods for segmenting the tumor part.

We analyze the complexity of the proposed method with the region grow and Singh and Dubey method. Table III below shows the calculation of time complexity in seconds performed on MATLAB 10, Intel 2.40GHz, with memory 2.0GB. From the table below, it is clear that the time taken to run the proposed method is less than the other two methods. Therefore, we can say that the proposed method has less time complexity in comparison to the region grow and Singh and Dubey method and the proposed method outperforms the other two methods.

TABLE III. TIME COMPLEXITY

Figure	Proposed	Region grow	Singh and Dubey
Fig. 3	2.99	4.3	4.83
Fig. 4	2.39	4.23	5.01
Fig. 5	2.23	4.75	5.05
Fig. 6	2.13	5.10	4.34
Fig. 7	3.04	4.55	5.19

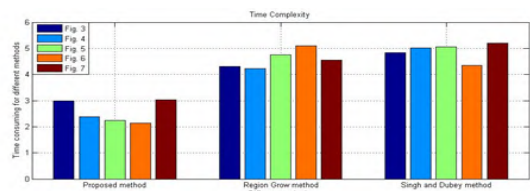


Fig. 9. Time complexity calculated for proposed and other two methods.

V. CONCLUSION AND FUTURE WORK

In this paper, an efficient method for the extraction of brain tumor has been introduced. The proposed method is based on Zernike moments. The high-order Zernike moments not only have very high computational complexity but they are even sensitive to noise. Therefore, the proper value should be chosen that is shown in the above table. Some values from the low-order Zernike moments are chosen, so that a high-order value does not have much effect during the computation of the mean value. The combination of mean values from the low and high-order Zernike moments is able to extract the tumor part from the different kinds of

brain tumor images invariant of its shape, size and intensity. The method proposed here is simpler and easy to understand. Even the proposed method is able to extract the tumor efficiently from the MR images; it also paves the way for the expert to decide whether the extracted brain tumor is benign and malignant due to many pathological features. This will be the subject of future research.

ACKNOWLEDGEMENTS

This research was supported by Basic Science Research Program through the National Research Foundation of Korea (NRF) funded by the Ministry of Education, Science and Technology (No.2010-0008974)

REFERENCES

- [1] V. Rajamani and S. Murugavalli, "A High Speed Parallel Fuzzy C-means Algorithm for Brain Tumor Segmentation," *ICGIST International Journal on BIME*, vol. 6, Dec. 2006, pp. 29-34
- [2] D. Vignion et al., "A New Method based on both Fuzzy set and Possibility Theories for Tumor Volume Segmentation on PET images," 30th International Conference of IEEE EMBS, Aug. 20-25, 2008, pp. 3122-3125.
- [3] S.M. Bhandarkar and P. Nammalwar, "Segmentation of Multispectral MR images Using a Hierarchical Self-Organizing Map Computer-Based Medical System CBMS 2001," *Proc. 14th IEEE Symposium*, vol 26, no. 27, 2001, pp. 294-299.
- [4] J. Chunyan, X. Zhang, W. Huang, and C. Meinel., "Segmentation and Quantification of Brain Tumor," *IEEE international Conference on Virtual Environment, Human-Computer Interfaces and Measurement Systems*, 2004, pp. 61-66.
- [5] Clark et al., "Automatic Tumor Segmentation using Knowledge based Techniques," *IEEE Transactions on Medical Imaging*, vol. 17, 1998, pp. 187-201.
- [6] Fletcher-Heath et al., "Automatic Segmentation of Non-enhancing Brain Tumor in MR Images," *Artificial Intelligence in Medicine*, vol. 21, 2001, pp. 43-63.
- [7] Kaus MR et al., "Segmentation of Meningiomas and Low Grade Gliomas in MRI," *MICCAI*, Cambridge, UK, 1999, pp. 1-10.
- [8] N. Moon, E. Bullitt, K. Leemput, and G. Greig, "Model-based Brain and Tumor Segmentation," *Proc. of ICPR*, Aug. 2002, pp. 528-531.
- [9] N. Otsu, "A Threshold Selection Method from Greylevel Histogram," *IEEE Transactions on System, Man and Cybernetic*, vol. 9, 1979, pp. 62-66.
- [10] M. Prastawa, E. Bullitt, S. Ho, and G. Gerig, "A Brain Tumor Segmentation Framework based on Outlier Detection," *Medical Image Analysis*, vol. 8, 2004, pp. 275-283.
- [11] AS. Capelle, O. Alata, C. Fernandez, S. Lefevre, and J.C. Ferrie, "Unsupervised Segmentation for Automatic Detection of Brain Tumors in MRI," *Proc. of Int. Conf. on Image Processing*, 2000, pp. 613-616.
- [12] MB. Caudra et al., "Atlas based Segmentation of Pathological Brains Using a Model of Tumor Growth," *MICCAI*, 2002, pp. 380-387.
- [13] F. Lefebvre, G. Berger, and P. Laugier, "Automatic Detection of the Boundary of the Calcarine from Ultrasound Parametric Images Using an Active Contour Model-Clinical Assessment," *IEEE Transactions on Medical Imaging*, vol. 17(1), 1998, pp. 45-52.
- [14] W. Wang, J.E. Mottershead, and C. Mares, "Mode-shape Recognition and Finite Element Model Updating Using the Zernike Moment Descriptor," *J. Mechanical Systems and Signal Processing*, vol. 23, 2009, pp. 2088-2112.
- [15] P. Gibbs, D. Buckley, S. Blackband, and A. Horsman, "Tumour Volume Determination from MR Images by Morphological Segmentation," *Physics in Medicine and Biology*, vol. 13, 1996, pp. 2437-2446.
- [16] J.K. Udupa, P.K. Saha, and R.A. Lotufo, "Relative Fuzzy Connectedness and Object Definition: Theory, Algorithms, and Applications in Image Segmentation," *IEEE Transactions on Pattern Analysis and Machine Intelligence*, vol. 24(11), 2002 pp. 1485-1500.
- [17] A. Khotanzad and Y.H. Hong, "Rotation Invariant Image Recognition Using Features Selected via a Systematic Method," *Pattern Recognition* vol. 23(10) , 1990, pp. 1089-1101.
- [18] S. Ghosal and R. Mehrotra, "Robust Optical Flow Estimation Using Semiinvariant Local Features," *Pattern Recognition*, vol. 30(2), 1997, pp. 229-237.
- [19] S.X. Liao and M. Pawlak, "On the Accuracy of Zernike Moments for Image Analysis," *IEEE Trans. Pattern anal. Mach. Intell.*, vol. 20, 1998, pp. 1358-1364.
- [20] R.R. Bailey and M. Srinath, "Orthogonal Moment Features for use with Parametric and Non-parametric Classifiers," *IEEE Trans. Pattern anal. Mach. Intell.*, vol. 18, 1996, pp. 389-400.
- [21] S.K. Hwang and W.Y. Kim, "A Novel Approach to the Fast Computation of Zernike Moments," *Pattern Recognition*, vol. 39, 2006, pp. 2065-2076.
- [22] Sh. Li, M.Ch. Lee, and Ch.M. Pun, "Complex Zernike Moments Features for Shape-based Image Retrieval," *IEEE Transactions on Systems, Man and Cybernetics, Part A: Systems and Humans*, vol. 1 (39), 2009, pp. 227-237.
- [23] X. Li and A. Song, "A New Edge Detection Method Using Gaussian-Zernike Moment Operator," In *Proceedings of the IEEE, 2nd International Asia Conference on Informatics in Control*, vol. 1, March, 2010, pp. 276-279.
- [24] J. Haddadnia, M. Ahmadi, and K. Faez, "An Efficient Feature Extraction Method with Pseudo-Zernike Moment in RBF Neural Network-based Human Face Recognition System," *Journal of Applied Signal Processing*, vol. 9, 2003, pp. 890-901.
- [25] Z. Iscan, Z. Dokur, and T. Olmez, "Tumor Detection by Using Zernike Moments on Segmented Magnetic Resonance Brain Images," *Expert Systems with Application*, vol. 37, 2010, pp. 2540-2549.
- [26] A. Tahmasbi, F. Saki, and S. B. Shokouhi, "Classification of Benign and Malignant Masses based on Zernike Moments," *Computers in Biology and Medicine*, vol. 41, 2011, pp. 726-73
- [27] L. Singh, R.B. Dubey, and Z.A. Jaffery, "Segmentation and Characterization of Brain Tumor from MR Images," *Proc. Int. on Advances in Recent Technologies in Communication and Computing*, 2009, pp. 815-819.
- [28] K. Thapaliya and G.R. Kwon, "Extraction of Brain Tumor Based on Morphological Operations," *Proc. Int. ICCM*, vol. 1, 2012, pp. 515-520.
- [29] P.Narendran, V.K Narendira Kumar, K. Somasundaram, "3D Brain Tumor and Internal Brain Structures Segmentation in MR Images," *IJ Image, Graphics and Signal Processing*, vol. 1, 2012, pp-35-43